

The hypotaurine-aurine pathway as an antioxidative mechanism in patients with acute liver failure

Takamasa Mizota,^{1,†} Takako Hishiki,^{2,†} Masahiro Shinoda,^{1,3,*} Yoshiko Naito,² Kazuya Hirukawa,¹ Yohei Masugi,⁴ Osamu Itano,⁵ Hideaki Obara,¹ Minoru Kitago,¹ Hiroshi Yagi,¹ Yuta Abe,¹ Kentaro Matsubara,¹ Makoto Suematsu,² and Yuko Kitagawa¹

¹Department of Surgery, ²Department of Biochemistry, and ⁴Department of Pathology, Keio University School of Medicine, 35 Shinanomachi, Shinjuku-ku, Tokyo 160-8582, Japan

³Digestive Diseases Center, International University of Health and Welfare Mita Hospital, 1-4-3 Mita, Minato-ku, Tokyo 108-8329, Japan

⁵Department of Hepato-Biliary-Pancreatic and Gastrointestinal Surgery, International University of Health and Welfare School of Medicine, 4-3 Kozunomori, Narita, Chiba 286-0124, Japan

(Received 15 April, 2021; Accepted 19 April, 2021; Released online in J-STAGE as advance publication 26 June, 2021)

The liver has been thought to protect against oxidative stress through mechanisms involving reduced glutathione (GSH) that consumes high-energy phosphor-nucleotides on its synthesis. However, hepatoprotective mechanisms in acute liver failure (ALF) where the phosphor-nucleotides are decreased in remain to be solved. Liver tissues were collected from patients with ALF and liver cirrhosis (LC) and living donors (HD) who had undergone liver transplantation. Tissues were used for metabolomic analyses to determine metabolites belonging to the central carbon metabolism, and to determine sulfur-containing metabolites. ALF and LC exhibited a significant decline in metabolites of glycolysis and pentose phosphate pathways and high-energy phosphor-nucleotides such as adenosine triphosphate as compared with HD. Conversely, methionine, S-adenosyl-L-methionine, and the ratio of serine to 3-phosphoglycerate were elevated significantly in ALF as compared with LC and HD, suggesting a metabolic boost from glycolysis towards trans-sulfuration. Notably in ALF, the increases in hypotaurine (HTU) + taurine (TU) coincided with decreases in the total amounts of reduced and oxidized glutathione (GSH + 2GSSG). Plasma NH₃ levels correlated with the ratio of HTU + TU to GSH + 2GSSG. Increased tissue levels of HTU + TU vs total glutathione appear to serve as a biomarker correlating with hyperammonemia, suggesting putative roles of the HTU-TU pathway in anti-oxidative protective mechanisms.

Key Words: acute liver failure, glutathione, hyperammonemia, hypotaurine, metabolome analysis

Acute liver failure (ALF) is a clinical syndrome characterized by progressive and massive hepatocellular necrosis.⁽¹⁾ Despite recent therapeutic advances, ALF remains a serious clinical condition that is associated with a high mortality rate.⁽²⁾ Previous studies have suggested that oxidative stress plays a crucial role in the mechanisms of liver injury in ALF.⁽³⁾ Under physiological conditions, the liver is protected from oxidative stress by the capacity of its hepatocytes to generate reduced glutathione (GSH), the synthesis of which is dependent on adenosine triphosphate (ATP),⁽⁴⁾ and its oxidized form (GSSG), which is recycled back to the reduced form using reduced nicotinamide adenine dinucleotide phosphate (NADPH) provided by the pentose phosphate pathway (PPP). However, it remains unclear as to how hepatoprotective mechanism operates during ALF, in which the energy metabolism is compromised. It is therefore important to investigate alterations in high energy

phosphor-nucleotides and antioxidative metabolites by determining the levels of all metabolites, and to examine which metabolic pathways respond specifically to ALF. Such approaches could provide valuable insight into the specific metabolic responses in ALF patients and ultimately assist in the development of therapeutic approaches to control liver failure. To this end, we applied a metabolomic approach to determine metabolites in liver tissues under conditions of ALF and liver cirrhosis (LC) relative to healthy donors (HD).

While metabolomics has widely been used to determine tissue metabolites associated with experimental models of drug-induced or ischemic liver injury,⁽⁵⁻⁸⁾ few studies provided data collected from human liver tissues under disease conditions. In this study, we collected liver samples from hepatectomized ALF patients, as well as patients with LC and HD subjects, and analyzed them using 2 different metabolomic approaches: one involves capillary electrophoresis mass spectrometry (CE-MS) to analyze central carbon metabolism, amino acid metabolism, and phosphor-nucleotides as energy substrates. Since reductive metabolites such as GSH and hypotaurine (HTU) are prone to artificial modification during sample handling and measurements, we utilized liquid chromatography mass spectrometry (LC-MS) to determine GSH and HTU under conditions in which artificial modification of these metabolites is minimized *in vitro*. A serendipitous observation in this study was that, in ALF, an increased level of HTU + taurine (TU) coincided with decreases in the total amount of glutathione (GSH + 2GSSG), suggesting relative enhancement of the HTU-TU pathway for anti-oxidative defense mechanisms.

Methods

Patients. This study included 8 patients with ALF (ALF group) (2 living-donor liver transplantation patients and 6 deceased-donor liver transplantation patients), 13 patients with LC (LC group) (12 living-donor liver transplantation patients and 1 deceased-donor liver transplantation patients), and 12 healthy living donors (HD group). Patients with hepatitis were diagnosed as having ALF when they developed at least grade II hepatic encephalopathy due to severe liver damage, as represented by prothrombin times $\leq 40\%$ of the standardized value, within 8

[†]Equally contributed authors.

^{*}To whom correspondence should be addressed.

E-mail: masa02114@yahoo.co.jp

weeks of the onset of hepatitis symptoms.^(9,10) All patients with ALF or LC were judged to be eligible for liver transplantation due to end-stage liver disease by the Institutional Committee for Liver Transplantation Indication at Keio University School of Medicine. Subjects in the HD group were certified to be in a good health by the committee based on systemic examination including liver function tests and liver imaging. Resected liver samples were pathologically examined if the findings were morphologically comparable to the preoperative diagnosis.

Informed consent was obtained from each patient or their family, and the study protocol conformed to the ethical guidelines of Keio University School of Medicine (authorization number: 20130400).

Hepatic tissue sampling. Liver samples were collected from the native liver immediately after total hepatectomy in patients with ALF and LC. For the donor operation, an intraoperative liver biopsy was performed at the beginning of the operation to determine whether the liver was pathologically normal and qualified for grafting.⁽¹¹⁾ A small part of the intraoperative liver biopsy specimen of the donors was collected from HD subjects. Hepatic tissue samples were immediately frozen in liquid nitrogen. Hepatic tissue samples were also examined histologically to confirm whether pathological findings were compatible to the preoperative diagnosis.

Data collection from medical records. The following parameters were retrospectively assessed using medical records; age, sex, etiology of diseases, blood test data [aspartate aminotransferase (AST), alanine aminotransferase (ALT), total bilirubin (TB), albumin, prothrombin time-international normalized ratio (PT-INR), creatinine, NH₃, and platelet counts] and model for end-stage liver disease (MELD) score.^(12,13) Blood test data obtained immediately before liver transplantation were used. The MELD score was calculated using the following equation, as described previously,^(12,13) with data for TB, PT-INR, and creatinine obtained immediately before transplantation: MELD score = $9.57 \times [\log_e(\text{creatinine})] + 3.78 \times [\log_e(\text{TB})] + 11.2 \times [\log_e(\text{PT-INR})] + 6.43$.^(12,13)

Measurement of liver metabolites by CE-MS. CE-MS was conducted as previously described.^(14–20) Frozen liver samples were quickly weighed without thawing and 10 mg portions were prepared for CE-MS analysis. The samples were then plunged into ice-cold methanol (500 μ l) containing internal standards (300 μ M L-methionine sulfone for cations and 300 μ M morpholinoethane sulfonic acid for anions) and crushed using a tissue disruptor (Multi-Beads Shocker; Yasui Kikai, Osaka, Japan). A 250 μ l aliquot of ultrapure water (LC-MS grade; Wako, Osaka, Japan) was added to the sample and 750 μ l of the resulting solution was combined with 500 μ l of chloroform and mixed thoroughly. The suspension was centrifuged at 15,000 g for 15 min at 4°C. The upper aqueous layer was extracted again using chloroform and was centrifugally filtered through a 5-kDa cutoff filter (UFC3LCCNB; Human Metabolome Technologies, Tsuruoka, Japan) to remove proteins. The filtrate was concentrated with a vacuum concentrator (SpeedVac; Thermo, Yokohama, Japan) which helps in quantitating trace levels of metabolites. The concentrated filtrate was dissolved in 200 μ l ultrapure water containing reference compounds (200 μ M 3-aminopyrrolidine and 200 μ M trimesate) before the CE-MS analysis. Quantification of the metabolites was performed using a capillary electrophoresis system (Agilent Technologies, Tokyo, Japan) equipped with an air pressure pump, a mass spectrometer (1,200 series), an isocratic high-performance liquid chromatography pump (G1603A CE/MS adapter kit), and a spray unit (G1607A). System control, data acquisition, and evaluation were conducted using commercial software for CE-MS (G2201AA Agilent ChemStation). Differences in the levels of liver metabolites were compared among the groups.

Measurements of TU, HTU, GSH, and GSSG levels by LC-MS. TU, HTU, GSH, and GSSG were measured using a Nexera UHPLC system coupled with LC-MS 8030plus triple quadrupole mass spectrometer (Shimadzu, Kyoto, Japan). Separation was achieved using an Acquity UPLC BEH amide column (1.7 μ m, 2.1 \times 150 mm; Waters, Milford, MS). The mobile phase consisted of water containing 0.1% formic acid (A) and acetonitrile containing 0.1% formic acid (B). The following gradient program was used: 0–1 min, 95% B; 1–3 min, 77% B; 3–11 min, 75% B; 11–14 min, 25% B; 14–20 min, 15% B; 20–21 min, 95% B; and held for 4 min. The injection volume was 2 μ l. The column oven was kept at 40°C and the flow rate was set to 0.2 ml/min. Optimization of multiple reaction monitoring (MRM) transition for the compounds was performed automatically using the built-in algorithm of the LCMS-8030plus; the optimized MRM transitions were m/z 124.00>79.80 for TU, m/z 611.25>306.1 for GSSG, m/z 194.05>79.90 for 2-morpholinoethanesulfonic acid (an internal standard) in negative mode, and m/z 109.85>30.10 for HTU, m/z 308.10>179.05 for GSH in positive mode. The interface ionization potential was set at 4.5 kV with a temperature of 400°C. The flow rates of nebulizer and drying gases were set at 1.5 and 10 L/min, respectively.

Correlation analysis between clinical parameters and the ratio of HTU + TU to GSH + 2GSSG. We analyzed the correlation between the ratio of HTU + TU vs GSH + 2GSSG and clinical parameters such as age, blood test data (AST, ALT, TB, albumin, PT-INR, creatinine, NH₃, and platelet count), and MELD score in the LC and ALF groups.

Statistical analysis. Results are expressed as mean \pm SE. Statistical analyses were performed using one-way analysis of variance (ANOVA) and Fisher's least significant difference test for multiple comparisons. Correlations were evaluated using the Spearman rank test. Differences were considered statistically significant at p values less than 0.05.

Results

Patient characteristics. Patient characteristics are shown in Table 1. Pathological findings were compatible to the preoperative diagnoses in all subjects. Representative pathological findings are shown in Fig. 1.

Metabolomic profiling of liver analyzed by CE-MS. Figure 2 shows data for phosphor-nucleotides, their derivatives, and the energy charge (EC) index. With respect to nicotinamide adenine dinucleotide (NAD) and nicotinamide adenine dinucleotide phosphate (NADP), the levels of their reduced forms (NADH, NADPH) and oxidized forms (NAD, NADP), and the ratio of the reduced to oxidized forms were significantly or markedly decreased in LC and ALF liver as compared with HD liver. The EC index [ATP + 1/2 adenosine diphosphate (ADP)]/[adenosine monophosphate (AMP) + ADP + ATP] was also significantly decreased in LC and ALF liver relative to HD liver.

Figure 3 shows alterations in glycolysis, tricarboxylic acid (TCA) cycle, PPP, fatty acid metabolism, serine/glycine cleavage system, methylation cycle, trans-sulfuration pathway, and urea cycle. In the glycolysis pathway, the sum of all metabolites was significantly lower in LC and ALF liver than in HD liver. The levels of acetyl CoA, a metabolite in the TCA cycle, were significantly lower in ALF and LC liver than in HD liver, while the level of lactate was significantly higher in ALF and LC than in HD liver. The levels of all PPP metabolites were decreased in LC and ALF vs HD liver. Distinct from downstream glycolytic intermediates such as 3-phosphoglycerate (3PG) and phosphoenolpyruvate (PEP), most of the upstream glycolytic intermediates were lower in LC and ALF vs HD, and consequently the sum of glycolytic intermediates (Σ glycolysis in Fig. 3) displayed significant decreases in LC and ALF liver. The significant decrease in acetyl CoA in LC and ALF but not in HD

suggests an overburden in glycolysis in LC and ALF.

Among the metabolites examined, several exhibited alterations specifically in ALF but not in LC. At least 3 different metabolic pathways appeared to be altered in ALF: First, free amino acid pools were elevated with marginally significant changes presumably because of catabolism induced by protein degradation.⁽²¹⁾ As discussed below, ALF displayed elevation of serum level of NH₃ (Table 1) and resultant elevation of citrulline (Fig. 3), suggesting the presence of catabolism. Secondly, remethylation cycle metabolites showed significant elevation of *S*-adenosyl-L-methionine (SAM) and methionine. The third one was a significant elevation of the ratio of serine vs 3PG; which is a marker indicative of consumption of 3PG to generate serine. To be noted, trans-sulfuration metabolites displayed marked alterations: significant elevations of cystathionine and HTU levels were observed while the level of GSH was not significantly elevated. These changes observed in ALF suggest that elevation of free amino acids including methionine and serine, and the up-regulation of HTU belonging to trans-sulfuration metabolites are events that occur selectively in ALF but neither in LC nor HD.

LC-MS analyses for GSH-GSSG and HTU-TU in ALF. Quantitative determination of GSH and HTU requires careful technical attention to get rid of artificial modification of these metabolites during sample processing and analyses *in vitro*.⁽²²⁾ We thus used LC-MS to determine these metabolites.⁽²²⁾ As shown in Fig. 4, the levels of GSH, GSSG, and GSH + 2GSSG were significantly decreased in ALF liver. Conversely, the levels of HTU were modestly but not significantly increased in LC and ALF. TU was significantly elevated in LC and ALF. Consequently, HTU + TU levels were significantly elevated in LC and ALF liver. Considering that glutathione and taurine share the same substrates such as cystathionine and cysteine to be synthesized, these results suggest utilization of anti-oxidative metabolites appears distinct between ALF and the two other groups. To compare relative importance of these different antioxidant systems, we calculated the ratio of HTU + TU to GSH + 2GSSG [(HTU + TU)/(GSH + 2GSSG)] for the individual groups. As shown in Fig. 4C, the

ratio was significantly higher in ALF than in LC and HD.

Since the severity of ALF may differ among individual cases in the ALF group, we examined the correlation between the (HTU + TU)/(GSH + GSSG) values and other clinical parameters. The correlation coefficients and *p* values (in parentheses) between the ratio of HTU + TU/GSH + 2GSSG and parameters in the LC group were; age, R = 0.361 (*p* = 0.226); AST, R = 0.158 (*p* = 0.606); ALT, R = 0.014 (*p* = 0.963); TB, R = 0.333 (*p* = 0.266); albumin, R = 0.329 (*p* = 0.272); PT-INR, R = 0.147 (*p* = 0.633); creatinine, R = 0.244 (*p* = 0.422); MELD score, R = 0.084 (*p* = 0.784) in the LC group. In the ALF group, the values were: age, R = 0.495 (*p* = 0.212); AST, R = 0.361 (*p* = 0.379); ALT, R = 0.257 (*p* = 0.538); TB, R = 0.272 (*p* = 0.515); albumin, R = 0.093 (*p* = 0.826); PT-INR, R = 0.266 (*p* = 0.525); creatinine, R = 0.035 (*p* = 0.935); MELD score, R = 0.566 (*p* = 0.144). For NH₃, the values were R = 0.156 (*p* = 0.612) in the LC group and R = 0.708 (*p* = 0.049) in the ALF group. Figure 5 shows the correlation between the ratio of HTU + TU to GSH + 2GSSG and NH₃ in LC and ALF cases. There was a significant correlation between the ratio of HTU + TU/GSH + 2GSSG and plasma NH₃ levels for ALF but not LC. The MELD score, another marker indicating the severity of liver failure, showed no significant correlation with the ratio of (HTU + TU)/(GSH + 2GSSG).

Discussion

The current study revealed alterations in metabolic systems of the human liver undergoing ALF. Such alterations in ALF included significant elevation of the ratio of HTU + TU to GSH + 2GSSG. To date, several studies on metabolic profiling in ALF have been carried out in animal models and in human sera. Soga and colleagues⁽⁸⁾ employed CE-MS to determine liver metabolites in a mouse ALF model. Analyzing serum samples, they reported that serum ophthalmate is a biomarker for oxidative stress. Also employing a mouse ALF model, Feng and colleagues used gas chromatography mass spectrometry (GC-MS) to profile liver metabolites in liver tissue and found significant changes

Table 1. Patient characteristics

	HD (n = 12)	LC (n = 13)	ALF (n = 8)
Age (years)	43.3 ± 4.2	55.5 ± 2.4*	44.5 ± 5.1 [†]
Gender (male/female)	7/5	7/6	4/4
Etiology of disease			
Hepatitis C virus	—	4	0
Primary biliary cholangitis	—	4	0
Alcohol	—	3	0
Autoimmune hepatitis	—	1	2
Wilson disease	—	0	1
Unknown	—	1	5
Blood test data			
AST (IU/L)	19.9 ± 1.0	66.2 ± 8.4**	67.9 ± 15.9**
ALT (IU/L)	22.0 ± 2.4	39.2 ± 4.9**	51.3 ± 8.5**
TB (mg/dl)	0.8 ± 0.1	7.2 ± 2.1**	15.8 ± 2.5** [†]
Albumin (g/dl)	4.50 ± 0.10	2.42 ± 0.11**	3.24 ± 0.19** ^{††}
Creatinine (mg/dl)	0.79 ± 0.05	0.87 ± 0.10	0.61 ± 0.06*
Platelet count (×10 ⁴ /μl)	23.1 ± 1.1	7.9 ± 1.3**	6.0 ± 0.9**
PT-INR	0.98 ± 0.01	1.54 ± 0.12**	2.33 ± 0.17** ^{††}
NH ₃ (μg/dl)	N/A	48.5 ± 10.0	70.4 ± 11.4
MELD score	6.0 ± 0.0	18.6 ± 2.1**	32.4 ± 3.5** ^{††}

Values represent the number of cases or mean ± SE. HD, healthy donor; LC, liver cirrhosis; ALF, acute liver failure; TB, total bilirubin; PT-INR, prothrombin time-international normalized ratio; MELD, model for end-stage liver disease. **p* < 0.05 vs HD. ***p* < 0.01 vs HD. [†]*p* < 0.05 vs LC. ^{††}*p* < 0.01 vs LC.

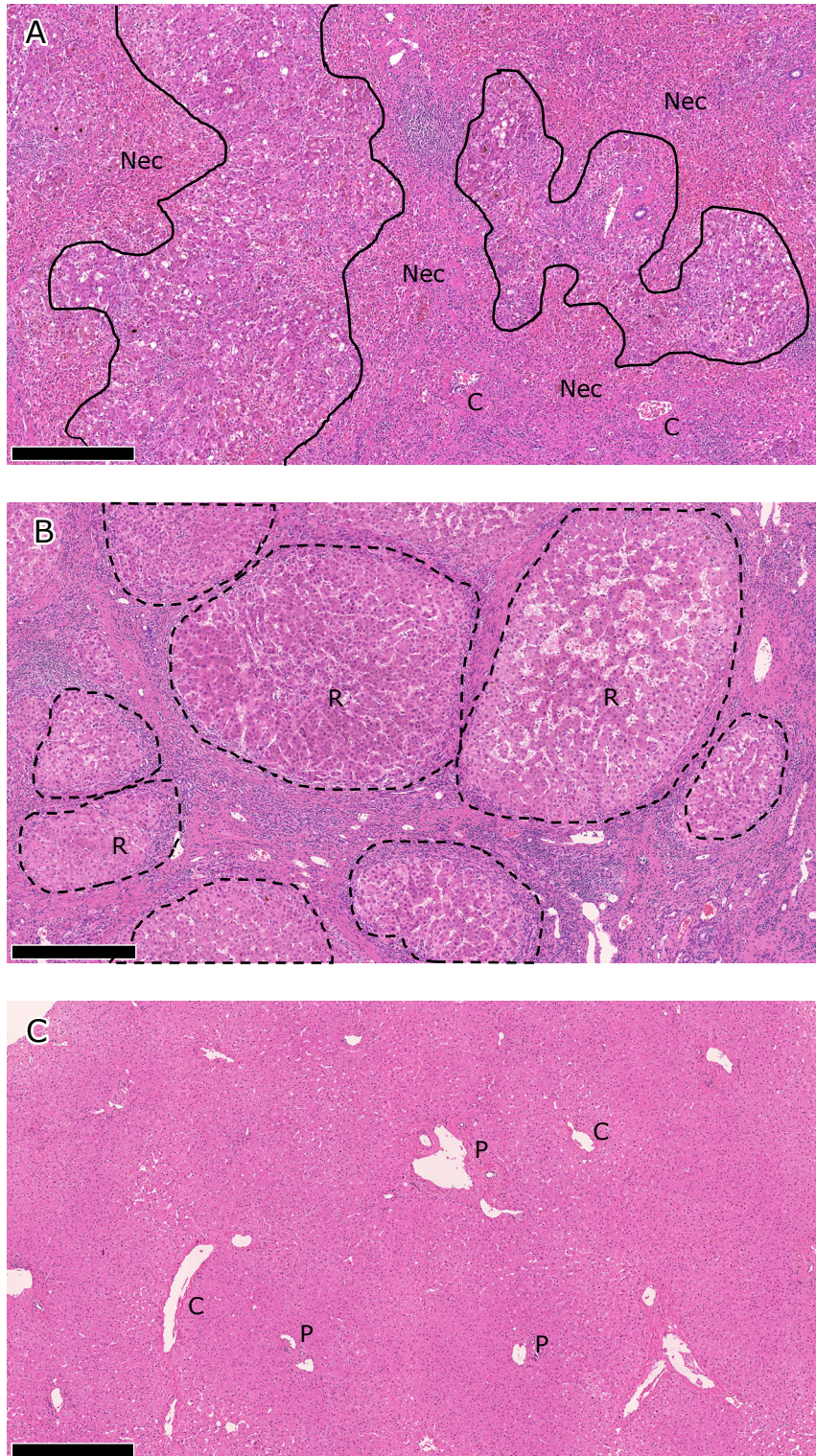


Fig. 1. Pathological findings in A) ALF, B) LC, and B) HD livers. Representative findings are shown for each liver disease category. The scale bar represents 500 µm. A) Hepatocytes have been extensively destroyed to form bridging/panlobular necrotic areas (Nec), where collapsed hemorrhagic stroma, inflammatory cell infiltrates, and ductular reactions are seen. Native structures of the liver, including the portal venules (P) and central venules (C), are preserved. B) Liver structures are totally remodeled in the cirrhotic liver, which is characterized by nodules of regenerating hepatic parenchyma (R, regenerative nodules). Regenerative nodules are separated by dense fibrous septum with vascular vessels and inflammation. C) Intact portal venules (P) and central venules (C) are embedded in hepatic parenchyma in the normal liver. ALF, acute liver failure; LC, liver cirrhosis; HD, healthy donor.

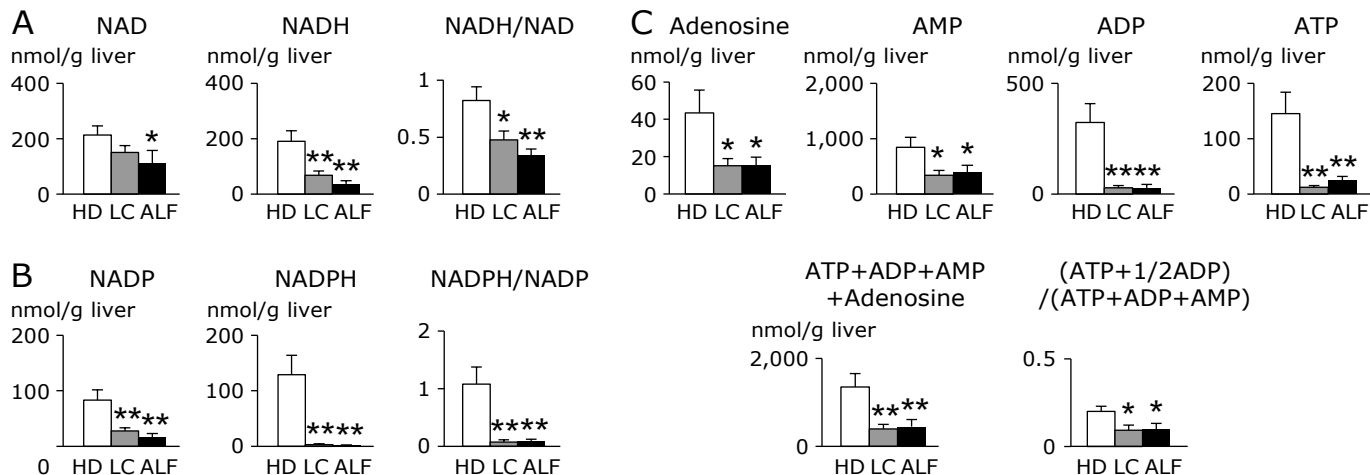


Fig. 2. Alterations in A) NAD(H), B) NADP(H), and C) adenosine and adenosine phosphates in liver from HD, LC and ALF subjects. The clear, stippled, and black bars represent HD, LC, and ALF groups, respectively. There were no significant differences between LC and ALF in any metabolites. * $p < 0.05$ vs HD. ** $p < 0.01$ vs HD. HD, healthy donor; LC, liver cirrhosis; ALF, acute liver failure; NAD, oxidized nicotinamide adenine dinucleotide; NADH, reduced nicotinamide adenine dinucleotide; NADP, oxidized nicotinamide adenine dinucleotide phosphate; NADPH, reduced nicotinamide adenine dinucleotide phosphate; AMP, adenosine monophosphate; ADP, adenosine diphosphate; ATP, adenosine triphosphate.

in many metabolites in ALF mice.^(5,6) Nie and colleagues⁽²³⁾ employed LC-MS to determine serum metabolites of patients with acute on chronic liver failure, and found that 17 metabolites were related to the prognosis of patients. However, all previous studies used animal samples or human sera and had limited ability to clarify the pathophysiological mechanisms involved in ALF patients. To our knowledge, this is the first study utilizing a metabolomic approach to examine multiple metabolites simultaneously in human liver tissues. In fact, this study identified a new biomarker and uncovered an antioxidative defense mechanism in ALF as described below.

This study also revealed that LC and ALF patients had markedly different levels of metabolites in the liver compared with HD subjects. First, NAD, NADP, and ATP were significantly reduced in LC and ALF compared with HD liver. NAD(H) and NADP(H) are essential reducing equivalents for maintaining energy metabolism and reductive biosynthesis, respectively. As compared with HD, ALF and LC displayed significant depression of energy metabolism as seen in Fig. 2. However, the current results uncovered differences between LC and ALF with respect to metabolite alterations.

Use of CE-MS-based metabolomics is beneficial for simultaneously pinpointing the response of multiple metabolic pathways under disease conditions. The CE-MS data shown in Fig. 3 shows that several metabolites were significantly elevated or reduced in ALF relative to LC or HD. Interestingly, the affected metabolites included L-carnitine, citrulline, methionine, the ratio of serine/3PG, SAM, and the ratio of SAM/S-adenosyl-L-homocysteine (SAH). It has been known that under physiological conditions the liver maintains its energy through fatty acid beta-oxidation and the urea cycle. A significant depletion of L-carnitine and accumulation of citrulline in ALF raises the possibility that there may be a failure of the liver to maintain ATP through these mechanisms. Diminished glycolytic intermediates (Σ glycolysis) also suggests that during ALF, the liver fails to produce energy from glycolysis. Despite these circumstances, the levels of metabolites of 3PG, serine, and methionine were maintained even in ALF. An increased ratio of serine/3PG indicates that central carbon units were preferentially supplied towards serine-glycine cleavage and possibly even to trans-sulfuration pathways.⁽²²⁾ In parallel with this supply, increased metabolites belonging to the remethylation cycle, reflected by

SAM and the ratio of SAM/SAH, also occurred in ALF liver. These lines of evidence led us to use LC-MS analyses to determine whether antioxidant metabolites belonging to the trans-sulfuration pathway such as glutathione and HTU-TU are up-regulated in ALF.

LC-MS analyses revealed that the $\text{HTU} + \text{TU}/\text{GSH} + 2\text{GSSG}$ ratio can serve as an index reflecting metabolic events that take place specifically in ALF. There is a critical difference between the anti-oxidative mechanisms of the GSH and HTU systems. Considering its concentration in the liver (several mM), the GSH-GSSG system provides one of the most prevalent anti-oxidative systems in the liver. However, the processes leading to GSH synthesis consume 2 ATP molecules, and recycling GSSG into GSH requires NADPH provided by the PPP.⁽²⁴⁾ ALF, in which the levels of PPP substrates and NADPH are reduced, might hinder the efficiency of the GSH system making it less robust. On the other hand, HTU synthesis and oxidation require neither ATP nor NADPH. Thus, HTU serves as a suicidal antioxidant which is readily oxidized into TU under oxidative stress, and is thus advantageous for protecting the liver under acute pathological conditions such as ALF. It is not unreasonable to suggest that the HTU-TU system serves as an energy-saving antioxidant mechanism not only in experimental models of rodents,⁽⁷⁾ but also in ALF of clinical cases.

We also found that the $(\text{HTU} + \text{TU})/(\text{GSH} + 2\text{GSSG})$ ratio showed a positive correlation with NH_3 levels. It is noteworthy that this new marker correlated with commonly used clinical parameters of severe liver failure. The urea cycle is one of the important mechanisms of NH_3 detoxification, but the reaction from NH_3 to carbamoyl phosphatase and the urea cycle itself are ATP-dependent. Accumulation of citrulline was confirmed in ALF as shown in Fig. 3. It is possible that markers which depends on the presence of energy correlate with one another. It was also interesting that the new marker did not correlate with other clinical parameters such as the MELD score and the levels of TB, prothrombin, and albumin. We assume that the correlation between a blood marker and a hepatic tissue marker can be affected by various factors such as whether the marker rapidly reflects an event in the tissue, is liver-specific, or undergoes modification such as blood transfusion.

This study elucidated an alternative antioxidative mechanism in the energy-deficient environment of ALF patients. No studies

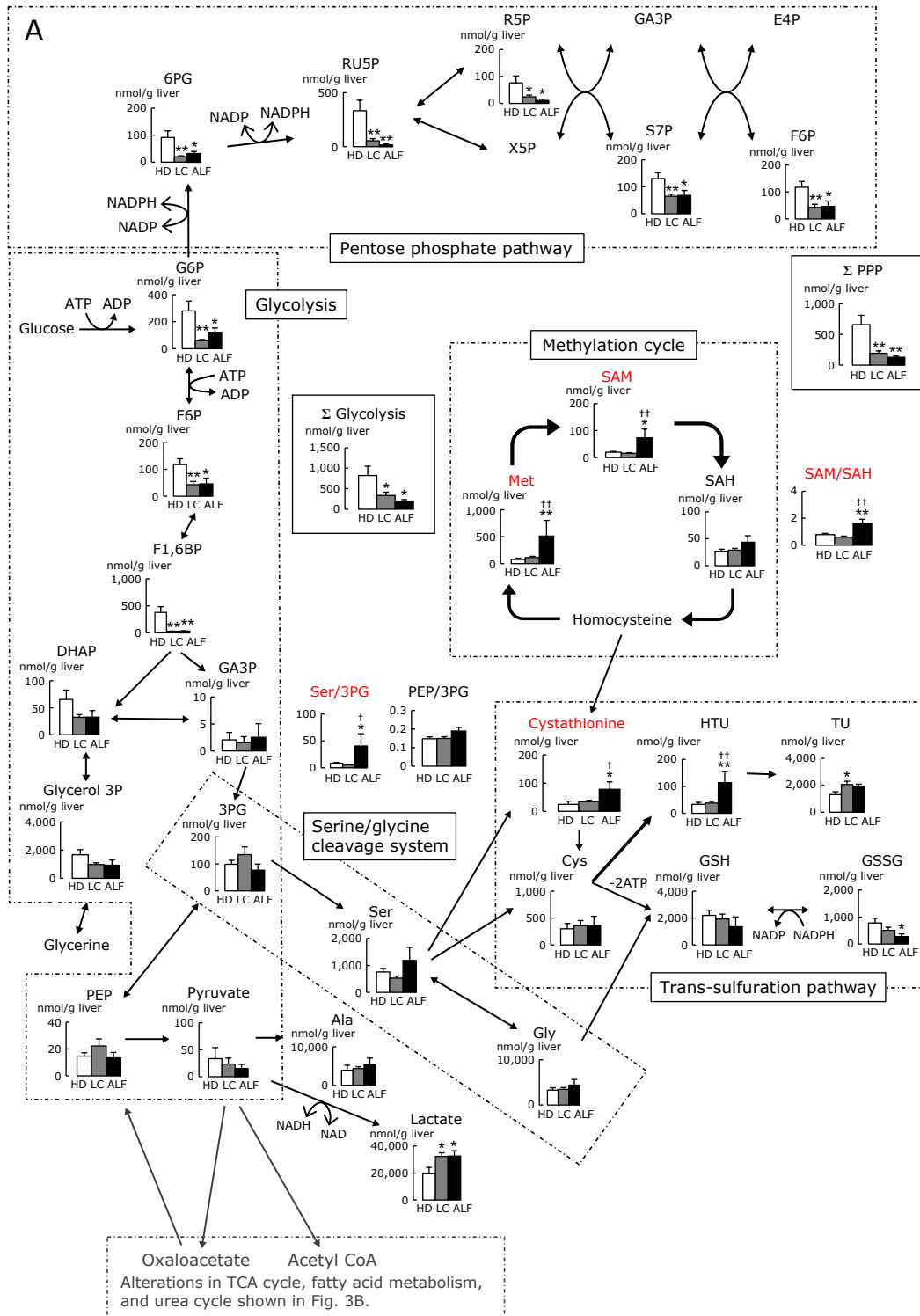


Fig. 3. Alterations in A) glycolysis, PPP, serine/glycine cleavage system, methylation cycle, and trans-sulfuration pathway, and B) TCA cycle, fatty acid metabolism, and urea cycle (analysis of CE-MS), in liver from HD, LC and ALF subjects. Note that the 2 figures A) and B) are connected between PEP-pyruvate and oxaloacetate-acetyl CoA. Clear, stippled, and black bars represent HD, LC, and ALF groups, respectively. * $p < 0.05$ vs HD. ** $p < 0.01$ vs HD. † $p < 0.05$ vs LC. †† $p < 0.01$ vs LC. HD, healthy donor; LC, liver cirrhosis; ALF, acute liver failure; TCA, tricarboxylic acid; PPP, pentose phosphate pathway; CE-MS, capillary electrophoresis mass spectrometry; NAD, oxidized nicotinamide adenine dinucleotide; NADH, reduced nicotinamide adenine dinucleotide; NADP, oxidized nicotinamide adenine dinucleotide phosphate; NADPH, reduced nicotinamide adenine dinucleotide phosphate; ATP, adenosine triphosphate; ADP, adenosine diphosphate; AMP, adenosine monophosphate; G6P, glucose 6-phosphate; F6P, fructose 6-phosphate; F1,6BP, fructose 1,6-diphosphate; DHAP, dihydroxyacetone phosphate; GA3P, glyceraldehyde 3-phosphate; 3PG, 3-phosphoglycerate; PEP, phosphoenolpyruvate; 6PG, 6-phosphogluconate; RU5P, ribulose 5-phosphate; R5P, ribose 5-phosphate; S7P, D-sedoheptulose 7-phosphate; X5P, xylulose 5-phosphate; E4P, erythrose 4-phosphate; SAM, S-adenosyl-L-methionine; SAH, S-adenosyl-L-homocysteine; HTU, hypotaurine; TU, taurine; GSH, reduced glutathione; GSSG, oxidized glutathione.

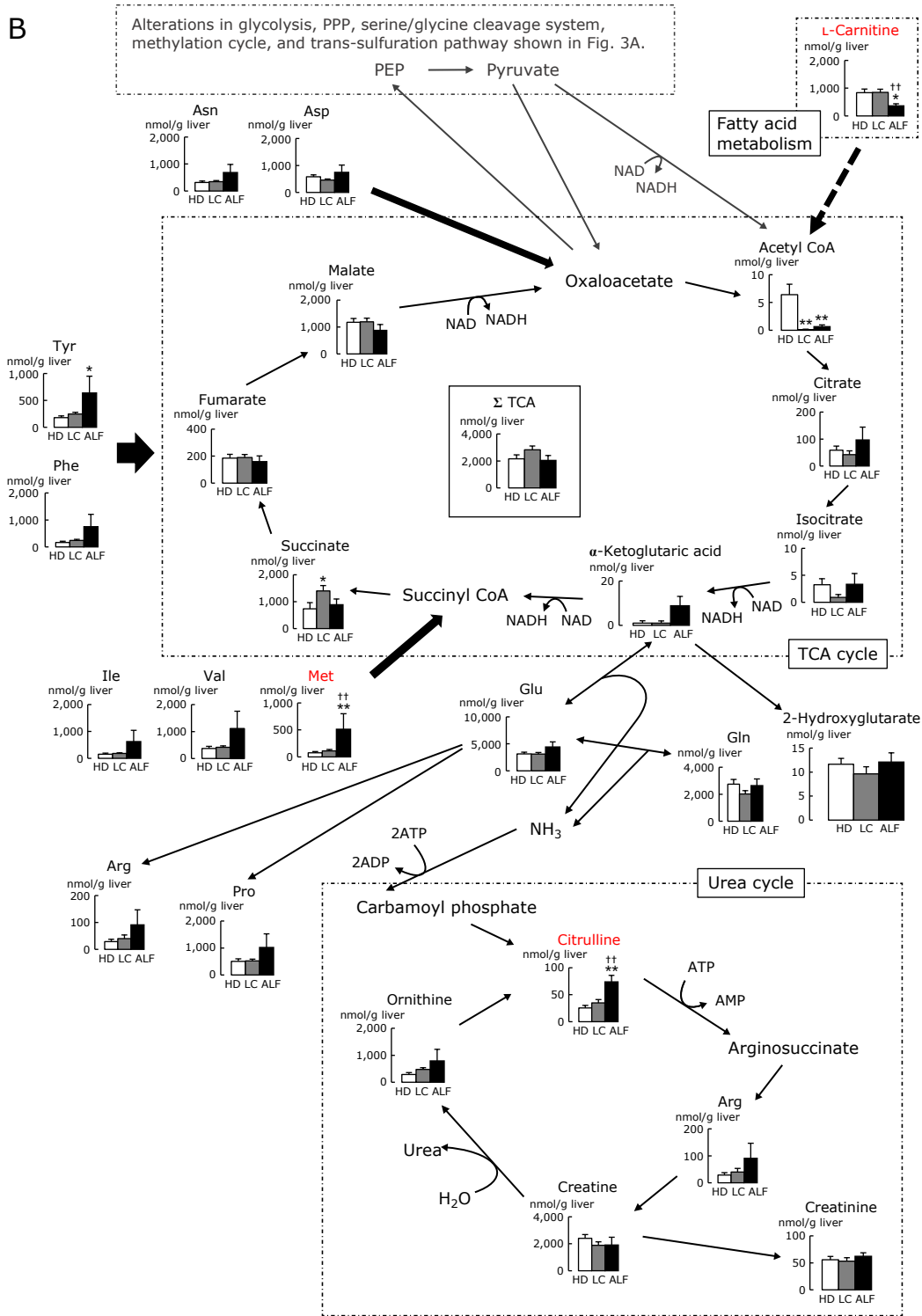


Fig. 3. continued

on ALF or acute on chronic liver failure have previously identified the HTU + TU/GSH + 2GSSG ratio as a biomarker.^(5,6,8,23) Interestingly, a similar alternative metabolism was reported in ischemia-reperfusion injury. Sakuragawa and colleagues⁽⁷⁾ applied CE-MS in a rat model of hepatic ischemia-reperfusion. They reported that TU serves as a surrogate marker for ischemia-reperfusion and that HTU acts as an energy-saving hepatoprotective

amino acid in the model. It is possible that the alternative metabolic pathway, in which the HTU-TU redox mechanism predominates over the GSH-GSSG redox mechanism, is commonly employed in diseases associated with an oxidant-rich environment or energy deficiency.

In conclusion, the current clinical observation shed light on the critical role of the HTU-TU system as compared with the GSH-

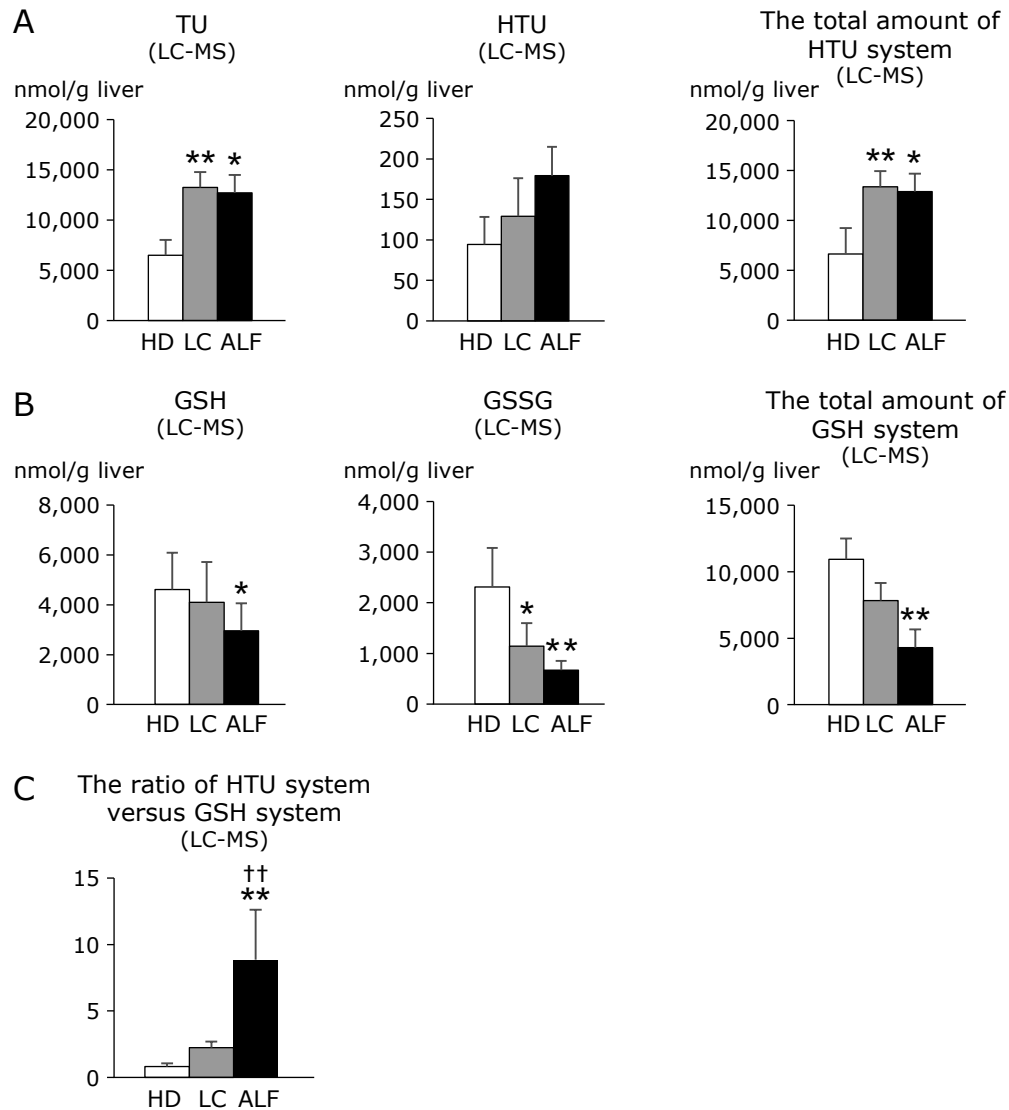


Fig. 4. Alterations in A) the metabolites in the HTU system and the total amount of HTU system, B) the metabolites in the GSH system and the total amount of GSH system, and C) the ratio of HTU system vs GSH system in liver from HD, LC and ALF subjects (LC-MS analysis). Clear, stippled, and black bars represent HD, LC, and ALF groups, respectively. The total amount of HTU system is calculated as HTU + TU. The total amount of GSH system is calculated as GSH + 2GSSG because a GSSG molecule derives from 2 GSH molecules. The ratio of HTU system vs GSH system is calculated as HTU + TU/GSH + 2GSSG. * $p < 0.05$ vs HD. ** $p < 0.01$ vs HD. † $p < 0.05$ vs LC. †† $p < 0.01$ vs LC. Note that the levels of TU and HTU + TU are significantly increased in LC and ALF compared with HD, while the levels of GSH and GSSG are markedly decreased in LC and ALF compared with HD. There was no significant difference between LC and ALF. The (HTU + TU)/(GSH + 2GSSG) ratio was significantly increased in ALF as compared with HD and LC. LC-MS, liquid chromatography mass spectrometry; HD, healthy donor; LC, liver cirrhosis; ALF, acute liver failure; HTU, hypotaurine; TU, taurine; GSH, reduced glutathione; GSSG, oxidized glutathione.

GSSG system as a protective mechanism in patients with ALF. In rodent experiments, HTU administered into the circulation increases the amounts of HTU and TU in liver tissues and attenuates ischemia-reperfusion injury.⁽⁷⁾ Further studies are necessary to determine whether supplementation of HTU and/or TU can result in improvement of clinical outcomes in ALF patients.

Author Contributions

TM, TH, and MS performed the research design, data analysis, figure creation, and manuscript preparation. TM and TH equally contributed to this article as first authors. YN participated in measurement of metabolites. YM participated in pathological interpretation. KH participated in medical data collection. OI,

HO, MK, HY, YA, and KM were engaged in the treatment of patients. MS and YK participated in the research design and conducted the project.

Acknowledgments

We would like to thank the late Professor Masaki Kitajima, MD, PhD for his enthusiastic support of our project and clinical research on liver transplantation.

Abbreviations

ADP adenosine diphosphate
ALF acute liver failure
ALT alanine aminotransferase

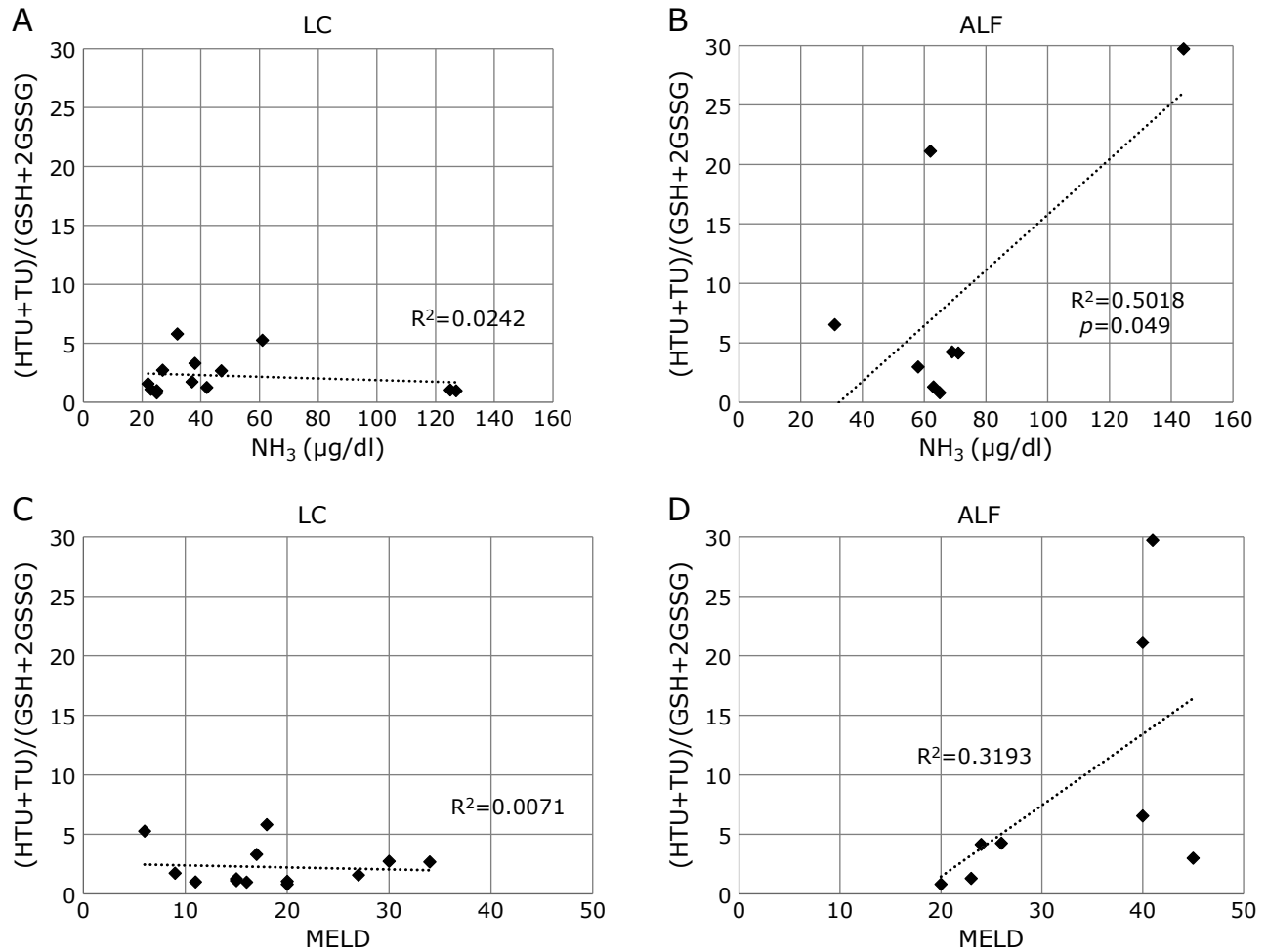


Fig. 5. Correlation between the ratio of HTU + TU to GSH + 2GSSG and NH₃ in A) LC and B) ALF groups, and between the ratio of HTU + TU to GSH + 2GSSG and MELD score in C) LC and D) ALF groups. The ratio of HTU + TU to GSH + 2GSSG and NH₃ levels showed a high positive correlation in ALF but no correlation in LC. LC, liver cirrhosis; ALF, acute liver failure; HTU, hypotaurine; TU, taurine; GSH, reduced glutathione; GSSG, oxidized glutathione; MELD, model for end-stage liver disease.

AMP adenosine monophosphate
 AST aspartate aminotransferase
 ATP adenosine triphosphate
 CE-MS capillary electrophoresis mass spectrometry
 EC energy charge
 GC-MS gas chromatography mass spectrometry
 GSH reduced glutathione
 GSSG oxidized glutathione
 HD healthy donor
 HTU hypotaurine
 LC liver cirrhosis
 LC-MS liquid chromatography mass spectrometry
 MELD model for end-stage liver disease
 MRM multiple reaction monitoring
 NAD oxidized nicotinamide adenine dinucleotide
 NADH reduced nicotinamide adenine dinucleotide

NADP oxidized nicotinamide adenine dinucleotide phosphate
 NADPH reduced nicotinamide adenine dinucleotide phosphate
 PEP phosphoenolpyruvate
 3PG 3-phosphoglycerate
 PPP pentose phosphate pathway
 PT-INR prothrombin time-international normalized ratio
 SAH S-adenosyl-L-homocysteine
 SAM S-adenosyl-L-methionine
 TB total bilirubin
 TCA tricarboxylic acid
 TU taurine

Conflict of Interest

No potential conflicts of interest were disclosed.

References

- Oshima G, Shinoda M, Tanabe M, *et al.* Increased plasma levels of high mobility group box 1 in patients with acute liver failure. *Eur Surg Res* 2012; **48**: 154–162.
- Fujiwara K, Mochida S, Matsui A, *et al.* Fulminant hepatitis and late onset hepatic failure in Japan. *Hepatol Res* 2008; **38**: 646–657.
- McGill MR, Jaeschke H. Oxidative stress in acute liver failure. In: Albano E, Parola M, eds. *Studies on Hepatic Disorders*, New Jersey: Humana Press, 2015; 199–214.

- 4 Chen Y, Dong H, Thompson DC, Shertzer HG, Nebert DW, Vasiliou V. Glutathione defence mechanism in liver injury: insights from animal models. *Food Chem Toxicol* 2013; **60**: 38–44.
- 5 Feng B, Wu S, Liu F, Gao Y, Dong F, Wei L. Metabonomic analysis of liver tissue from BALB/c mice with D-galactosamine/lipopolysaccharide-induced acute hepatic failure. *BMC Gastroenterol* 2013; **13**: 73.
- 6 Feng B, Wu SM, Lv S, *et al.* A novel scoring system for prognostic prediction in d-galactosamine/lipopolysaccharide-induced fulminant hepatic failure BALB/c mice. *BMC Gastroenterol* 2009; **9**: 99.
- 7 Sakuragawa T, Hishiki T, Ueno Y, *et al.* Hypotaurine is an energy-saving hepatoprotective compound against ischemia-reperfusion injury of the rat liver. *J Clin Biochem Nutr* 2010; **46**: 126–134.
- 8 Soga T, Baran R, Suematsu M, *et al.* Differential metabolomics reveals ophthalmic acid as an oxidative stress biomarker indicating hepatic glutathione consumption. *J Biol Chem* 2006; **281**: 16768–16776.
- 9 Takahashi Y, Shimizu M. Aetiology and prognosis of fulminant viral hepatitis in Japan: a multicentre study. The Study Group of Fulminant Hepatitis. *J Gastroenterol Hepatol* 1991; **6**: 159–164.
- 10 Trey C. The fulminant hepatic failure surveillance study. Brief review of the effects of presumed etiology and age of survival. *Can Med Assoc J* 1972; **106** (Spec Issue): 525–528.
- 11 Shinoda M, Tanabe M, Itano O, *et al.* Left-side hepatectomy in living donors: through a reduced upper-midline incision for liver transplantation. *Transplant Proc* 2014; **46**: 1400–1406.
- 12 Kamath PS, Kim WR; Advanced Liver Disease Study Group. The model for end-stage liver disease (MELD). *Hepatology* 2007; **45**: 797–805.
- 13 Kamath PS, Wiesner RH, Malinchoc M, *et al.* A model to predict survival in patients with end-stage liver disease. *Hepatology* 2001; **33**: 464–470.
- 14 Yamazoe S, Naya M, Shiota M, *et al.* Large-area surface-enhanced Raman spectroscopy imaging of brain ischemia by gold nanoparticles grown on random nanoarrays of transparent boehmite. *ACS Nano* 2014; **8**: 5622–5632.
- 15 Yamamoto T, Takano N, Ishiwata K, *et al.* Reduced methylation of PFKFB3 in cancer cells shunts glucose towards the pentose phosphate pathway. *Nat Commun* 2014; **5**: 3480.
- 16 Takenouchi T, Sugiura Y, Morikawa T, *et al.* Therapeutic hypothermia achieves neuroprotection via a decrease in acetylcholine with a concurrent increase in carnitine in the neonatal hypoxia-ischemia. *J Cereb Blood Flow Metab* 2015; **35**: 794–805.
- 17 Shintani T, Iwabuchi T, Soga T, *et al.* Cystathionine beta-synthase as a carbon monoxide-sensitive regulator of bile excretion. *Hepatology* 2009; **49**: 141–150.
- 18 Morikawa T, Kajimura M, Nakamura T, *et al.* Hypoxic regulation of the cerebral microcirculation is mediated by a carbon monoxide-sensitive hydrogen sulfide pathway. *Proc Natl Acad Sci U S A* 2012; **109**: 1293–1298.
- 19 Matsuhashi T, Hishiki T, Zhou H, *et al.* Activation of pyruvate dehydrogenase by dichloroacetate has the potential to induce epigenetic remodeling in the heart. *J Mol Cell Cardiol* 2015; **82**: 116–124.
- 20 Hattori K, Kajimura M, Hishiki T, *et al.* Paradoxical ATP elevation in ischemic penumbra revealed by quantitative imaging mass spectrometry. *Antioxid Redox Signal* 2010; **13**: 1157–1167.
- 21 Clemmesen JO, Kondrup J, Ott P. Splanchnic and leg exchange of amino acids and ammonia in acute liver failure. *Gastroenterology* 2000; **118**: 1131–1139.
- 22 Shiota M, Naya M, Yamamoto T, *et al.* Gold-nanofève surface-enhanced Raman spectroscopy visualizes hypotaurine as a robust anti-oxidant consumed in cancer survival. *Nat Commun* 2018; **9**: 1561.
- 23 Nie CY, Han T, Zhang L, *et al.* Cross-sectional and dynamic change of serum metabolite profiling for Hepatitis B-related acute-on-chronic liver failure by UPLC/MS. *J Viral Hepat* 2014; **21**: 53–63.
- 24 Couto N, Malys N, Gaskell SJ, Barber J. Partition and turnover of glutathione reductase from *Saccharomyces cerevisiae*: a proteomic approach. *J Proteome Res* 2013; **12**: 2885–2894.



This is an open access article distributed under the terms of the Creative Commons Attribution-NonCommercial-NoDerivatives License (<http://creativecommons.org/licenses/by-nc-nd/4.0/>).